OPEN ACCESS

University of BRISTOL

Cullinan, J. F., Wisnom, M. R., & Bond, I. P. (2014). Damage manipulation & repair in composite T-joints. In *ECCM16 - 16th European Conference on Composite Materials: Seville, Spain, 22-26 June 2014* European Conference on Composite Materials, ECCM.

Peer reviewed version

Link to publication record in Explore Bristol Research
PDF-document

DAMAGE MANIPULATION & REPAIR IN COMPOSITE T-JOINTS

J. F. Cullinan[a*], M. R. Wisnom[a], I. P. Bond[a]

[a]Advanced Composites Centre for Innovation and Science (ACCIS), University of Bristol, Queens Building, University Walk, Bristol, BS8 1TR, United Kingdom
* Jack.Cullinan@Bristol.ac.uk

Keywords: Vasculature, Repair, T-Joint, Self-healing

Abstract
The purpose of this paper is to demonstrate a novel method for the intrinsic repair of sub critical damage in complex composite structures (T-joints). First, the failure modes of CRFP T-joints subject to static and fatigue loading were established and the influence of layup and interfacial ply orientation on failure was investigated. Based on these results, a number of strategies were proposed to mitigate the extent of damage during failure and subsequently implement an in-situ repair. The ability to isolate crack paths through the tailoring of interfacial ply orientation has been demonstrated. Finally, the ability to introduce repair 'infrastructure' in the form of hollow vasculature and thermoplastic interleaves, without influencing joint strength has been demonstrated.

1. Introduction

One of the key limitations of the use of composite materials in complex structures is their susceptibility to matrix dominated failure. Despite excellent in-plane axial performance, the strength of fibre reinforced polymers (FRPs) is often dictated by a relatively poor out of plane performance. Damage sustained during in-service use often manifests itself as microcracks within the matrix, which can coalesce to form intralaminar cracks or interlaminar delaminations. A major concern for designers is the presence of damage that is below the detectability threshold, but above the critical size for damage growth. In complex composite structures, particularly joints, detection of critical and sub-critical damage can be challenging. As a result a no growth philosophy is commonly adopted for composite design, often resulting in large safety factors being employed. Self-healing FRPs offer one potential solution to the problem of over-engineering of composite structures.

1.1. Self-healing Composite Materials

Inspired by the ability of biological systems to autonomously repair damage, a number of different approaches for implementing self-healing in man-made materials have been proposed. These can be broadly grouped into three different areas; discrete capsule based systems, continuous or semi-continuous vascular based systems and intrinsic systems. Capsule based systems were first proposed by White *et al.* [1] in 2001 and have since been adapted by a number of authors for introduction into fibre reinforce materials [2–4]. This method relies on the release of a healing agent into the damage zone and is currently a once off process as the functionality of the encapsulated healing agent cannot be restored. Vascular systems by contrast have the advantage of being able to continuously deliver agents to the

damage site and can be used for repeated healing. In this method a network of hollow channels known as vascules are placed within the structure and used for the introduction of a healing agent. A number of methods have been proposed for the introduction of these vascules, including the use of hollow glass fibres (HGFs), 3D printing, a 'lost wax' process and a solid preform route [5–9]. Intrinsic systems do not rely on a liquid phase healing agent; instead healing is achieved through chemical and physical interactions of the fracture plane post damage.

This paper will focus on the implementation of an intrinsic system in the form of EMAA interleaves and an extrinsic vascular system into FRPs. The ability to reliably ensure that fracture propagates through the embedded infrastructure will be demonstrated. Specifically this work aims to advance this technology through the TRL levels; extending current research into more industrially applicable complex structures and assessing performance under complex loading. Manufacturability, scale-up and industrialisation are three of the key considerations in the design and implementation of these systems. The term self-healing '*infrastructure*' is used here as a collective term to refer to the engineering features or inclusions in a material that provide a self-healing efficacy.

1.2. Composite T-joints

The T-joint geometry was selected for this investigation as it is commonly used in many composite applications and is a good lab-scale analogue for more complex structures. In aerospace structures this configuration is sometimes referred to as a 'T-piece' or 'T-section', as it is more commonly employed in turbine vanes, wing spars, and stiffened panels and not for secondary bonding of orthogonal structures as the name suggests. They are also commonly encountered in the marine industry, typically for the secondary bonding of discontinuous structures such as bulkheads and manifolds.
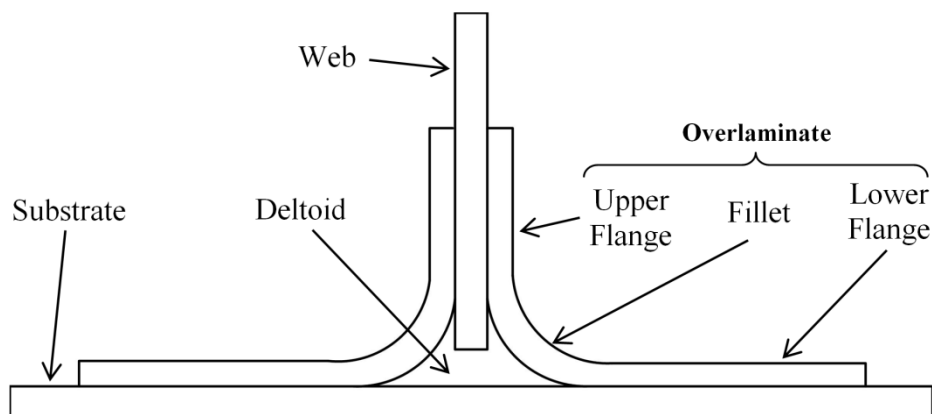
Figure 1. Schematic showing typical nomenclature for a webbed composite T-joint. A wide range of nomenclature has been used in literature to describe the various components of the T-joint geometry. For clarity this paper shall use the nomenclature outlined in the Figure above.

Failure of composite T-joints has been extensively investigated in literature for a variety of materials, loading conditions and design configurations. One of the primary failure modes identified is cracking of the deltoid region, followed by delamination of the overlaminate/substrate interface. This is generally the result of stress concentrations in the vicinity of the fillet radius and/or the relatively weak transverse strength of the deltoid material.

2. Experimental Procedure

2.1. Materials and Layup Configuration

Two joint types were examined during this investigation; 'aerospace grade' and 'marine grade'. Aerospace-grade joints were manufactured from IM7/8552 carbon epoxy prepreg tape (Hexcel, UK). The prepreg has a nominal sheet thickness of 0.125mm and is a typical aerospace grade composite material. The substrate and web plates were cured according to the manufacturer's specifications. The manufacturing procedure for the T-joints presented in this paper was adapted from a procedure outlined by Trask *et al*. [10]. A brief overview has been included here for completeness. Specimens were manufactured in a two-step process.

First, the substrate plate and web plate (if applicable) were layed up and fully cured. Two overlaminate L-sections were then laid up over a 10mm radius tooling. The deltoid region was manufactured by folding and consolidating a 90° ply of prepreg into a cavity formed by two touching 10mm radius aluminium blocks. PTFE coated metal wires (nominal OD = 0.52mm) were placed within the deltoid during layup. The overlaminates and deltoid were then co-cured between aluminium tooling blocks with substrate plate placed on top. If a web plate was used, this was sandwiched between the overlaminates during assembly and consolidated under vacuum. The layup for the various specimens is given in Table 1.

ID	Material	Ply Orientation			Infrastructure
		Substrate / Web	Overlaminate	Interface	
T1	IM7/8552	$[0°/-45°/90°/45°]_{3S}$	$[(0°/-45°/90°/45°)_2/0°]_S$	0°/0°	Control
T2	"	$[45°/0°/-45°/90°]_{3S}$	$[(\pm45°)_2/0°_4/90°_2/0°_4/(\pm45°)_2]_T$	±45°	5mm EMAA
T3	"	$[0°/-45°/90°/45°]_{3S}$	$[(0°/-45°/90°/45°)_2/0°]_S$	0°/0°	5mm EMAA
T4	"	"	"	"	A
T5	"	"	"	"	B
T6	"	"	"	"	C
T7	"	"	"	"	Web - Control
T8	"	"	"	"	Web & A

Table 1. Prepreg ply orientations and stacking sequences for T-joint specimens (where 0° corresponds to the primary loading direction of the web or vertical overlaminate as shown in Fig. 1).

For an overview of the positioning of the infrastructure within the deltoid please see Fig. 2(a) and Fig. 3. Polyethylene-co-methacrylic acid (EMAA) was selected as the interleave material of choice. Pellets of EMAA (15wt.% methacrylic acid, Sigma Aldrich) were hot pressed into sheets of 50µm nominal thickness and cut into 5mm strips. These strips were then placed immediately adjacent to each of the apexes in the deltoid region as shown in Fig. 2(a).

ID	Material	Ply Orientation			Infrastructure
		Substrate / Web	Overlaminate	Interface	
T9	T700/VTM 264	$[(0°/90°, \pm45°)_3 0°/90°]_S$	$[BX400]_2$	(0°/90°)/±45°	Web - Control
T10	"	"	"	"	Web & D
T11	T700/VTM 264/HP200	$[((0°/90°)/+45°/-45°), HP200]_S$	"	"	Web - Control
T12	"	"	"	"	Web & D

Table 2. Fibre orientations and stacking sequences for T-joint specimens (where 0° corresponds to the primary loading direction of the web or vertical overlaminate as shown in Fig. 1).

The investigation was extended to examine the potential application of this technology to marine-grade joints. Two webbed configurations were manufactured; a monolithic joint and a sandwich joint. In both cases the substrate and web plates were premanufactured before secondary bonding. Monolithic plates were made woven 2/2 twill carbon T700/VTM 264 epoxy prepreg (Cytec). The sandwich panels were made of a combination of woven and UD prepreg (also T700/VTM 264, Cytec) co-cured with 15mm Divinycell HP200 PVC/Polyurea foam core (Diab Group, Sweden). All plates were cured according to the manufacturer's recommendations. The layup for the various marine-grade specimens is given in Table 2.

An identical overlaminate layup procedure was used for both the monolithic and sandwich specimens. Web plates were mounted perpendicular to the substrate and adhered in place using a marine-grade thixotropic epoxy Spabond 340lv (Gurit, Switzerland). The epoxy was rounded to a 5mm radius using a circular scraper and left to cure fully. Vascules were created by embedding a Nylon 6/6 monofilament (nominal OD = 1mm) into the epoxy deltoid. After curing the surface was abraded using 120grit SiC abrasive paper, vacuumed and wiped with acetone. A marine-grade Resoltech 3350T/3357T structural adhesion promoter (Resoltech, France) was applied to the adherend surface before overlamination. Two layers of BX 400 carbon biaxial non crimp fabric (Formax, UK) were manually infiltrated with marine-grade Elan-tech EC152/W152 epoxy resin (Elantas, Italy) and bonded to the surface. The specimen was covered with P6 perforated release film and $150g/m^2$ breather clothe before being vacuum bagged and cured at room temperature before post curing at 50°C for 16 Hours.

The aerospace-grade specimens were cut to an overall length of 130mm and a nominal width of 20mm. The monolithic marine-grade joints were also manufactured to a nominal width and length of 20mm and 150mm respectively. Sandwich joints were cut to 25mm width and 180mm length. The height of the specimens was nominally 80mm for the aerospace joints and 120mm for the marine joints.

2.2. Test Procedure

Both static and fatigue tests were performed on an Instron 8872 servo-hydraulic test machine with hydraulic grips. Monolithic specimens were tested using a 10kN load cell, whilst tests on sandwich specimens were performed using a 5kN load cell. All tests were performed in tension by applying a pull off load to the vertical section (upper flange) of the overlaminate. The perpendicular section was constrained by two 10mm diameter loading rollers placed either 100mm (monolithic) or 130mm (sandwich) apart. The roller separation was increased from previous tests [10] to promote substrate bending and minimise experimental error associated with mounting of the specimens. Static tests were performed monotonically at 1mm/min until failure. Fatigue tests were performed under displacement control at either 50% (T9&T10) or 70% (T1-T8, T11&T12) of ultimate strength (frequency 4Hz, R=0.1) until failure of the specimen.

2.3. Numerical Modelling

The failure of T-joints has been well investigated analytically within the composites group at Bristol and as such a detailed numerical study is beyond the current scope of this work. It was still necessary however to qualitatively estimate the influence of vascule location on the stress state within the joint. A number of simple 3D linear elastic analyses were performed on the aerospace grade joints to determine the influence of vascule location using Abaqus/CAE 6.12. The analysis was based on previous work by Hélénon *et al.*[11] but limited to estimating

the linear stress response. FEA was not performed on the marine grade joints as failure was observed to be governed by inclusions within the overlaminate region, often inherent to wet layup manufacturing. Due to the stochastic nature of these inclusions, accurate prediction of apparent moduli and failure locations is difficult and beyond the scope of this work. Empirical observations of failure locations and crack propagation were preferred during this study.

## 3. Results & Discussion

3.1 Static Tests

Control tests performed on the monolithic aerospace T-joints revealed a variety of potential failure mechanisms. Failure appeared to initiate consistently at the deltoid/overlaminate interface, adjacent to the root of the overlaminate radius (fillet) section. This is to be expected as resin pockets at the 0°/90° interface of the deltoid, coupled with geometric stress concentrations provide favourable conditions for initial failure. Although initiation of damage within these specimens was well behaved, the propagation direction was observed to be somewhat stochastic. Four failure modes were identified; deltoid failure, overlaminate failure, substrate failure and interfacial failure, all of which rarely were present in isolation. In all cases (T1-T8) the flexural response of the joint was linear until failure. A typical load displacement response is given in Fig. 2(b).
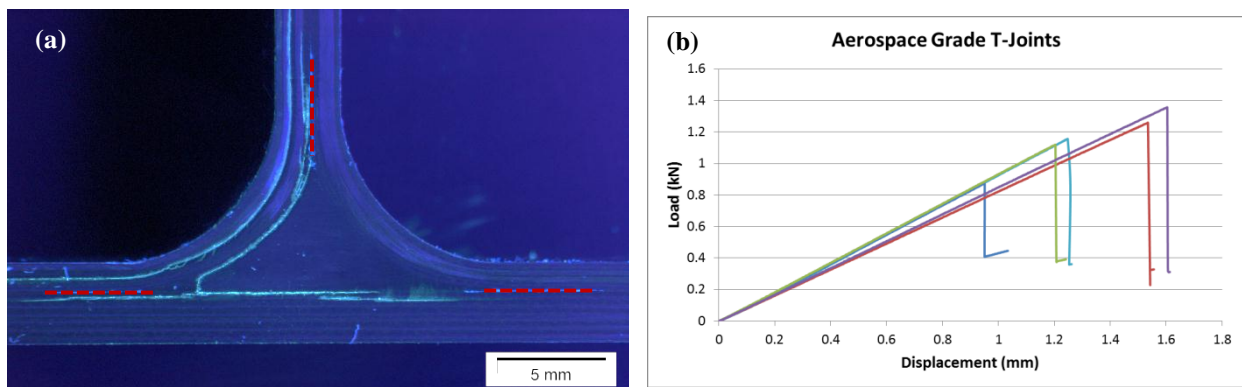

Figure 2. Typical failure of a composite T-joint (a) Stochastic failure mechanisms in T2, damage failed to propagate into interleaves (red) (b) Typical catastrophic failure of aerospace-grade joints (T4)

By adjusting the interfacial plies from ±45° to 0°/0° it was possible to prevent damage from propagating into the substrate and isolate failure within the interfacial plies. This was preferable as it was then possible to drive damage into EMAA interleaves as observed in T3. There was no statistical difference observed in failure load or flexural response from manipulation of the interfacial ply orientation.

It was important to determine an optimal location in which to place the vascules, such that reliable rupture occurred during testing and that the impact on static strength and fatigue life was minimised. Successful rupture of the vasculature was demonstrated in locations A, B & D. There was, however, a considerable knock down in static strength observed, whilst this was less pronounced in the T5 specimens (see Fig 4(a)). Using FEA it was determined that the proximity of location B to the 0° fibres in the overlaminate locally reduced max stresses at the periphery of the vascules. A third position, location C (T6), centrally located at the interface of the deltoid and substrate, has shown promise in FEA and is awaiting testing.
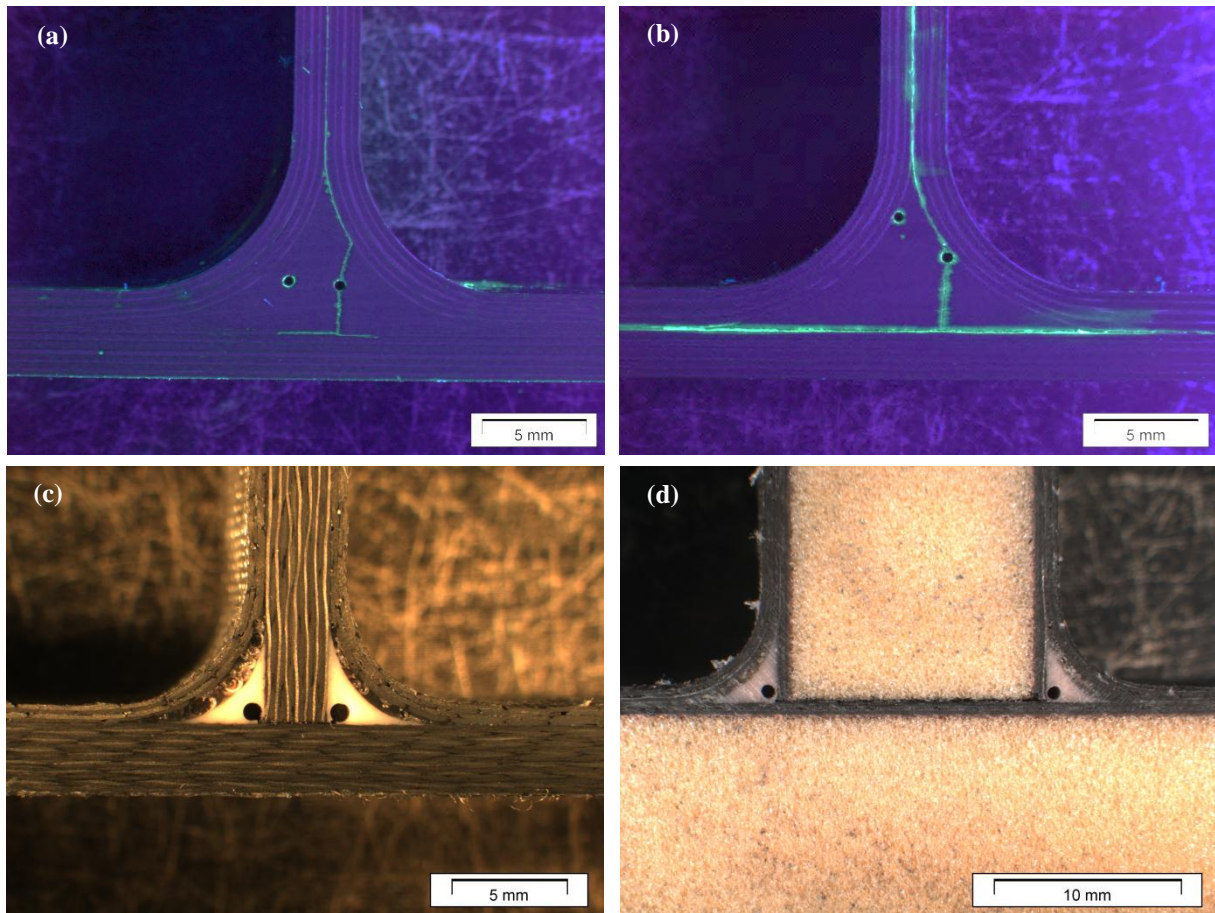
Figure 3. Vascularised specimens (a) Central vasculature, T4 (Aero-grade - Location A) (b) Vasculature at deltoid interface, T5 (Aero-grade - Location B) (c) Vasculature located at corner of web/substrate interface, T10 (Marine-grade - Location D) (d) Sandwich Structure, T12 (Marine-Grade - vascules at location D).
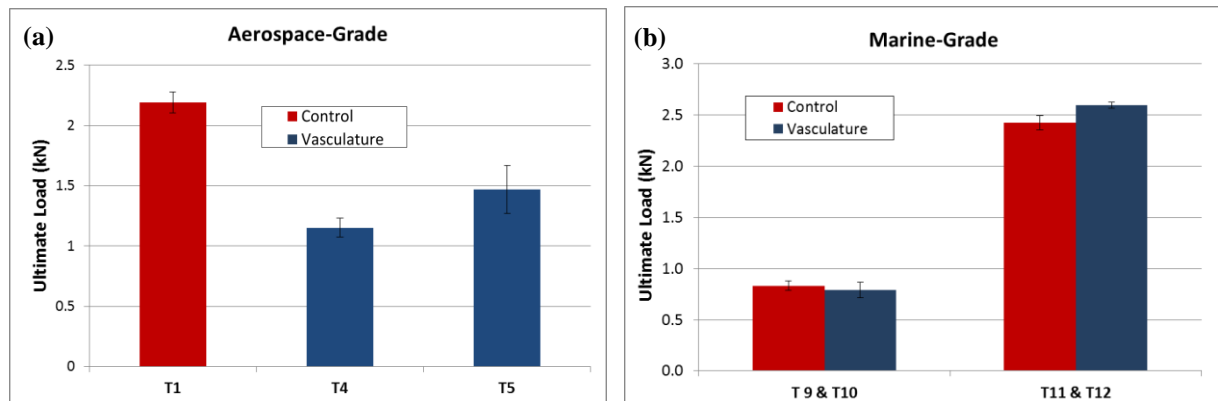
Figure 4. Ultimate loads at failure of T-joints. (a) Aerospace-grade joints (b) Marine-grade joints.

In contrast to the catastrophic failure of the unwebbed specimens, a more progressive failure mechanism was observed in webbed specimens of both aerospace (T7&T8) and marine grade (T9-T12) T-joints. Failure of the marine joints was two-fold; an initial load drop occurred when microcracks formed in the fillet region of the overlaminate. This damage then propagated and coalesced until a critical size was reached and catastrophic failure of the joint occurred. T9 & T10 both delaminated along the overlaminate/substrate interface, with the crack remaining planar and self-similar. T11 & T12 also failed in a similar manner, however, due to the low strain rate, core failure of the substrate was frequently observed. As can be

6

seen from Fig 4(b) there is no statistical influence of the presence of vasculature on the static strength of the T-joints.

3.2. Fatigue Tests

In general, fatigue failure mechanisms were observed to be macroscopically similar to the static failures. In T1-T6, stiffness degradation prior to catastrophic failure of the overlaminate interface was negligible or non-existent. In T3, damage was observed to successfully propagate through the EMAA interleaves, however, quantitatively determining their influence on crack propagation was difficult. Large scatter in the number of cycles to failure and the lack of sensible stiffness degradation also made the fatigue analysis of T4 & T5 difficult, however, there was a 100% success rate in the rupturing of vasculature.

By contrast, the webbed specimens T7 & T8 incurred almost instantaneous damage within the deltoid region, before progressive failure occurred as the overlaminate interfaces 'unzipped' in an apparent mode I manner. Micrographic analysis showed significant resin pockets in the deltoid regions, not typically observed in the unwebbed configuration, which may have promoted premature failure. It was speculated that this was likely to be an artefact of incomplete consolidation associated with having the deltoid region fully constrained between the aluminium tooling, web and substrate. A similar failure mechanism was observed in T9 & T12. Damage was instantaneous and initiated at the overlaminate/deltoid interface. As before, cracks continued to grow in a self-similar fashion through the overlaminate/substrate interface, prior to a secondary catastrophic failure event. Due to the higher strain rate, no core failures were observed in T11 or T12. In all cases the introduction of vasculature had no statistical effect on the number of cycles to failure or the onset of damage. There was a 100% success rate in the rupturing of vasculature in webbed specimens.

4. Conclusions

The ability to introduce two forms of self-healing infrastructure, interleaves and vascules, into a complex composite structure has been demonstrated using CFRP T-joints. Diffuse and stochastic damage was successfully controlled and directed towards embedded interleaves through tailoring of the interfacial ply orientation. Vasculature was introduced at various locations within an aerospace-grade T-joint and successfully ruptured under both static and fatigue loading. Early results showed a knock down in static strength of the order of 50%, however, this was reduced to 33% by varying the position of the vascules. FEA has been used to indicate that further improvements may be achieved through placement of vasculature at the deltoid/substrate interface. The concept was also successfully demonstrated in marine-grade T-joints. Damage was consistent in rupturing the vasculature and there was no effect on either the static strength or fatigue life of the joints tested.

Acknowledgements

References

[1]   S.R. White, N.R. Sottos, P.H. Geubelle, J.S. Moore, M.R. Kessler, S.R. Sriram, et al. Autonomic healing of polymer composites. *Nature*, 409:794–7, 2001.

[2]   M. Kessler, S. White. Self-activated healing of delamination damage in woven composites. Composites *Part A: Applied Science and Manufacturing*, 32:683–99,2001.

[3]   M Kessler, N Sottos, S.White. Self-healing structural composite materials. *Composites Part A: Applied Science and Manufacturing*, 34:743–53,2003.

[4]   T. O'Brien. Assesment of Composite Delamination Self-Healing Under Cyclic Loading. In *ICCM-17 17th International Conference on Composite Materials* 2009.

[5]   S.Bleay, C.Loader, V.Hawyes, L.Humberstone, P.Curtis A smart repair system for polymer matrix composites. *Composites Part A: Applied Science and Manufacturing*, 32:1767–76, 2001.

[6]   R.S. Trask, I.P.Bond, Biomimetic self-healing of advanced composite structures using hollow glass fibres. *Smart Materials and Structures*,15:704–10, 2006.

[7]   K.S. Toohey, N.R. Sottos, J. Lewis, J.S. Moore, S.R. White. Self-healing materials with microvascular networks. *Nature Materials*,6:581–5, 2007.

[8]   C-Y. Huang, R.S. Trask, I.P. Bond. Characterization and analysis of carbon fibre-reinforced polymer composite laminates with embedded circular vasculature. *Journal of the Royal Society, Interface / the Royal Society*,7:1229–41,2010.

[9]   A.P. Esser-Kahn, P.R. Thakre, H. Dong, J.F. Patrick, V.K. Vlasko-Vlasov, N.R. Sottos, *et al*. Three-dimensional microvascular fiber-reinforced composites. *Advanced Materials*, 23:3654–8, 2011.

[10]   R.S. Trask, S.R. Hallett, F.M.M. Helenon, M.R.Wisnom. Influence of process induced defects on the failure of composite T-joint specimens. C*omposites Part A: Applied Science and Manufacturing*,43:748–57, 2012.

[11]   F. Hélénon, M.R. Wisnom, S.R. Hallett, R.S. Trask. Numerical investigation into failure of laminated composite T-piece specimens under tensile loading. *Composites Part A: Applied Science and Manufacturing*,43:1017–27, 2012.